

Dendrimers Containing Organometallic Moieties Electronically Communicated

Isabel Cuadrado,^{*,†} Carmen M. Casado,[†] Beatriz Alonso,[†] Moisés Morán,[†] José Losada,[‡] and Vitaly Belsky[§]

Departamento de Química Inorgánica, Universidad Autónoma de Madrid, 28049-Madrid, Spain
Escuela Técnica Superior de Ingenieros Industriales Universidad Politécnica de Madrid, 28006-Madrid, Spain
Karpov Institute of Physical Chemistry, Vorontsov Pole 10 103064, Moscow, Russia

Received May 8, 1997

In the last few years, there has been a rapidly growing interest on metallocene-containing macromolecular materials in which metal atoms interact with one another.¹ On a different front, recent trends of research in dendrimers² have focused on the introduction of metal centers on the surface or within the dendritic structure.^{3,4} We recently reported silicon⁵ and amine-based⁶ dendrimers in which ferrocenyl moieties behave as electronically isolated units, and the dendritic molecules undergo a simultaneous multielectron transfer at the same potential. A challenging target is the construction of well-defined dendrimers possessing redox-active organometallic units linked together in close proximity so that there is electronic communication between the metal sites in the dendritic structure. This would provide access to new multimetallic dendrimers with appreciable electron mobility and consequently with interesting electrical, redox, optical, and magnetic properties.

We now report the convergent construction of novel dendrons and dendrimers possessing interacting ferrocenyl units. To our knowledge these are the first organometallic dendritic molecules displaying electronic interactions between transition metal atoms in the dendritic structure reported so far.

The key dendritic wedge for the synthesis of the new dendrimers is the silicon-bridged biferrocene **1** (Chart 1), which is prepared by reaction of ferrocenyllithium with vinylmethyl-dichlorosilane, in THF at $-20\text{ }^{\circ}\text{C}$. After purification, the target vinyl-terminated **1** was obtained as an orange crystalline solid. The molecular structure of **1** (Figure 1) shows that the ferrocenyl groups are oriented at ca. 90° relative to one another, and the

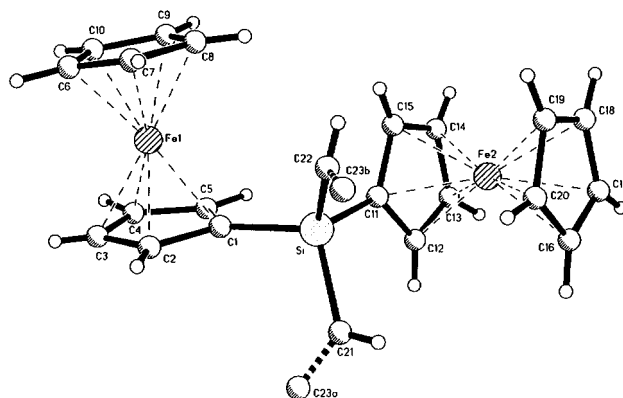
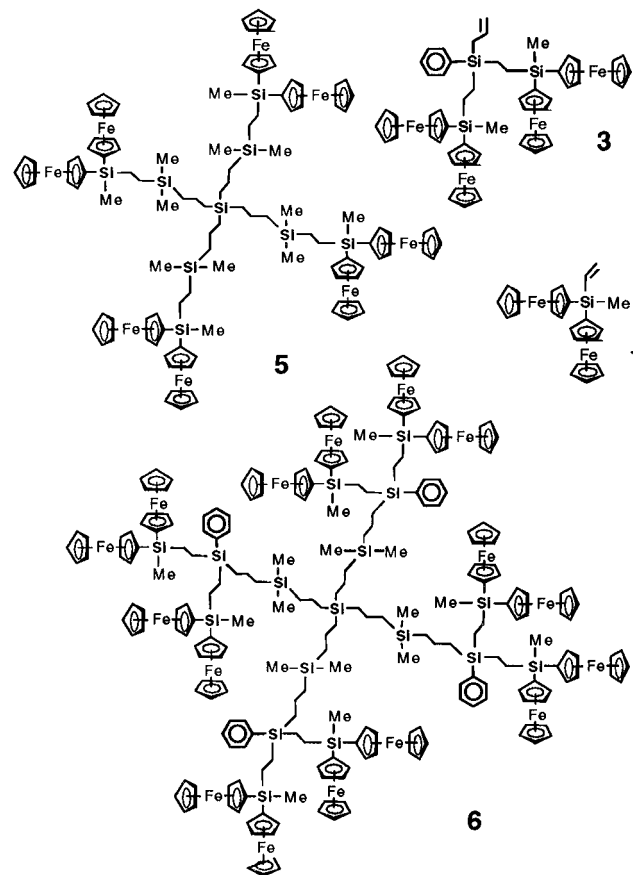


Figure 1. Crystal structure of dendron **1**. The methyl and vinyl groups are situated with statistic disorder (50% probability) around the silicon atom so that both C21 and C22 correspond to the disordered methyl and α -vinyl carbon atoms, while C23a and C23b correspond to the β -vinyl carbon atom (occupancy factor 0.5).

Chart 1



iron atoms are separated by 6.221 \AA .⁷ Further growth of this first-generation dendron was achieved by platinum-catalyzed hydrosilylation of **1** with phenylchlorosilane, resulting in the dendron $\text{ClSiPh}(\text{CH}_2\text{CH}_2\text{SiMeFc})_2$ (**2**), which contains a reactive chlorosilane functionality available for an ensuing alkenylation step. Treatment of **2** with allylmagnesium bromide, followed by hydrolytic workup afforded the desired growth dendron (**3**), carrying four ferrocenyl units.

The availability of the free carbon–carbon double bonds at the focal point of the dendritic wedges **1** and **3** enables the

(7) Crystal data for **1**: triclinic, $P\bar{1}$, $a = 7.5540(10)\text{ \AA}$, $b = 10.936(2)\text{ \AA}$, $c = 12.442(2)\text{ \AA}$, $\alpha = 101.330(10)^\circ$, $\beta = 84.580(10)^\circ$, $\gamma = 93.410(10)^\circ$, $V = 1002.4(3)\text{ \AA}^3$, $Z = 2$, $\mu = 1.510\text{ mm}^{-1}$, Mo $\text{K}\alpha$ radiation ($\lambda = 0.71073\text{ \AA}$), orange crystal ($0.35 \times 0.20 \times 0.20\text{ mm}$).

* E-mail: isabel.cuadrado@uam.es.

[†] Universidad Autónoma de Madrid.

[‡] Universidad Politécnica de Madrid.

[§] Karpov Institute of Physical Chemistry.

(1) See, for example: (a) Rulkens, R.; Lough, A. J.; Manners, I.; Lovelace, S. R.; Grant, C.; Geiger, W. E. *J. Am. Chem. Soc.* **1996**, *118*, 12683. (b) Pannel, K.; Dement'ev, V. V.; Li, H.; Cervantes-Lee, F.; Nguyen, M. T.; Diaz, A. F. *Organometallics* **1994**, *13*, 3644. (c) Brandt, P. F.; Rauchfuss, T. B. *J. Am. Chem. Soc.* **1992**, *114*, 1926. (d) Altmann, M.; Friedrich, J.; Beer, F.; Reuter, R.; Enkelmann, V.; Bunz, U. H. F. *J. Am. Chem. Soc.* **1997**, *119*, 1472.

(2) Recent reviews: (a) Newkome, G. R.; Moorefield, C. N.; Vögtle, F. *Dendritic Molecules: Concepts, Synthesis, Perspectives*; VCH: Weinheim, 1996. (b) Newkome, G. R. *Advances in Dendritic Macromolecules*; JAI Press: Greenwich, CT, 1994; Vol. 1, 1995; Vol. 2. (c) Fréchet, J. M. J. *Science* **1994**, *263*, 1710. (d) Ardoin, N.; Astruc, D. *Bull. Soc. Chim. Fr.* **1995**, *132*, 875.

(3) See, for example: (a) Valério, C.; Fillaut, J.-L.; Ruiz, J.; Guittard, J.; Blais, J.-C.; Astruc, D. *J. Am. Chem. Soc.* **1997**, *119*, 2588. (b) Bardaji, M.; Kustos, M.; Caminade, A.-M.; Majoral, J.-P.; Chaudret, B. *Organometallics* **1997**, *16*, 403. (c) Liu, G.-X.; Puddephatt, R. J. *Organometallics* **1996**, *15*, 5257. (d) Seyferth, D.; Kugita, T.; Rheingold, A.; Yap, G. P. A. *Organometallics* **1995**, *14*, 5362. (e) Bard, A. J. *Nature* **1995**, *374*, 374.

(4) Cuadrado, I.; Morán, M.; Losada, J.; Casado, C. M.; Pascual, C.; Alonso, B.; Lobete, F. In *Advances in Dendritic Macromolecules*; Newkome, G. R., Ed.; JAI Press: Greenwich, CT, 1996; Vol. 3, p 151.

(5) (a) Alonso, B.; Cuadrado, I.; Morán, M.; Losada, J. *J. Chem. Soc., Chem. Commun.* **1994**, 2575. (b) Alonso, B.; Morán, M.; Casado, C. M.; Lobete, F.; Losada, J.; Cuadrado, I. *Chem. Mater.* **1995**, *7*, 1440. (c) Losada, J.; Cuadrado, I.; Morán, M.; Casado, C. M.; Alonso, B.; Barranco, M. *Anal. Chim. Acta* **1996**, *251*, 5.

(6) Cuadrado, I.; Morán, M.; Casado, C. M.; Alonso, B.; Lobete, F.; García, B.; Ibsate, M.; Losada, J. *Organometallics* **1996**, *15*, 5278.

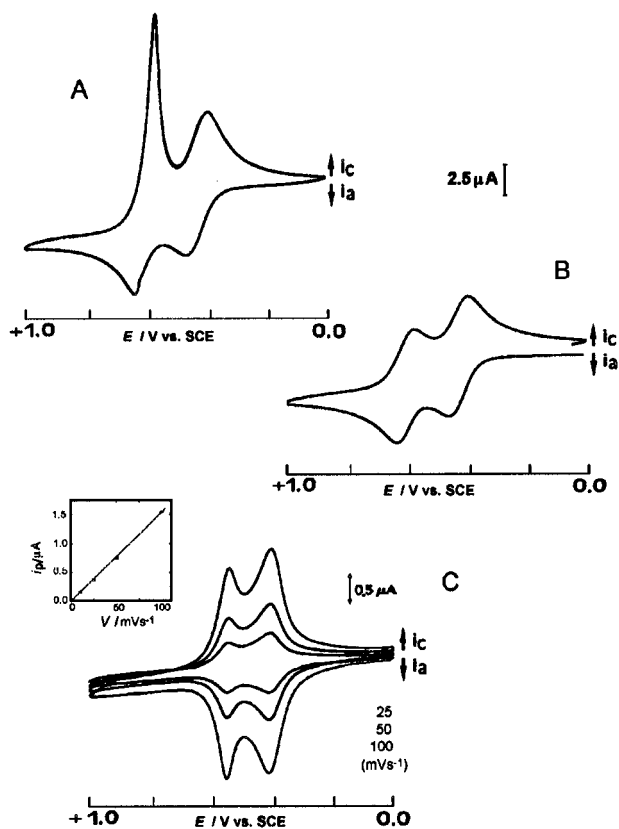


Figure 2. CVs of (A) **5** in CH_2Cl_2 , $E^\circ_1 = 0.42$, $E^\circ_2 = 0.59$ V vs SCE; (B) **5** in $\text{CH}_2\text{Cl}_2/\text{CH}_3\text{CN}$ (5:1 by volume), $E^\circ_1 = 0.41$, $E^\circ_2 = 0.60$ V vs SCE. Supporting electrolyte: 0.1 M TBAH; Pt disk electrode; scan rate 100 mV s^{-1} . (C) Voltammetric response of a Pt-disk electrode modified with a film of **5**, measured in $\text{CH}_2\text{Cl}_2/0.1 \text{ M TBAH}$. The surface coverage of the dendrimer was found to be $1.65 \times 10^{-10} \text{ mol cm}^{-2}$. Inset: Scan rate dependence of the first anodic peak current.

incorporation of interacting organometallic redox centers in dendritic structures through hydrosilylation reactions with Si–H polyfunctionalized cores, thus following a convergent approach. Hydrosilylation of **1** and **3** with the four-directional hydrosilane $[\text{Si}(\text{CH}_2)_3\text{Si}(\text{CH}_3)_2\text{H}]_4$ (**4**)⁴ afforded after chromatographic purification **5** and **6** (Chart 1) containing 8 and 16 ferrocenyl moieties on the dendritic surface, respectively.

The first and second generation dendritic wedges **1** and **3** function as valuable models with respect to the electrochemical properties of the corresponding dendrimers of higher nuclearity **5** and **6**. Both **1** and **3** exhibit cyclic voltammograms (CVs) in CH_2Cl_2 solution characterized by two well separated and reversible oxidation waves of equal intensity, at $E^\circ_1 = 0.45$ and $E^\circ_2 = 0.63$ V for **1** and 0.44 and 0.60 V (vs SCE) for **3**. A similar cyclic voltammetric response was observed for dendrimers **5** and **6**. Of interest, in CH_2Cl_2 with NBu_4PF_6 (TBAH) a change in solubility of **5** and **6** accompanied the change in oxidation state, so that the complete oxidation of both dendrimers appears to result in the precipitation of the oxidized dendrimers onto the electrode surface, and on the reverse scan the dendrimer redissolves as it is reduced (Figure 2A). In addition, upon continuous scanning in the potential range of 0

to +1 V vs SCE, an increase in the peak current with each successive scan was observed, indicating the formation of an electroactive film on the electrode surface. If a small amount of CH_3CN is added to the CH_2Cl_2 electrolyte medium, the cathodic stripping peak disappears (Figure 2B), and the CV of **5** and **6** becomes similar to that observed for **1** and **3**. Coulometry measurements after the complete oxidation resulted in the removal of 2 (for **1**), 4 (for **3**), 8 (for **5**), and 15.7 electron/molecule (for **6**). Likewise, differential pulse voltammetry (DPV) measurements for **1**, **3**, **5**, and **6** exhibited two separated oxidation waves of the same area.

The electrochemical behavior observed for these dendritic molecules is consistent with the existence of significant interactions between the two ferrocenyl units which are linked together by the bridging silicon atom.^{1a,b} The first oxidation of **1**, **3**, **5**, and **6** occurs in the dendritic wedges at nonadjacent ferrocene sites, which makes the subsequent removal of electrons from the remaining ferrocenyl centers, neighboring those already oxidized, more difficult. From the wave splitting ($\Delta E^\circ = E^\circ_2 - E^\circ_1$), which varies from $\Delta E^\circ = 190 \text{ mV}$ (for **5**) and 180 mV (for **1**), to $\Delta E^\circ \approx 160 \text{ mV}$ (for **3** and **6**), the comproportionation constant K_c relative to the equilibrium $\text{Fe(II)}-\text{Fe(II)} + \text{Fe(III)}-\text{Fe(III)} \rightleftharpoons 2\text{Fe(II)}-\text{Fe(III)}$ was calculated,⁸ resulting in values of $K_c = 1630$ for **5**, 1104 for **1**, and $K_c \approx 507$ for **3** and **6**. These values indicate that the partially oxidized dendritic molecules **1**, **3**, **5**, and **6** can be classified as class II mixed-valence species according to the Robin–Day classification.⁹

With **5** and **6** we have been able to prepare dendrimer-modified electrode surfaces. The voltammetric response of an electrodeposited film of dendrimer **5** is shown in Figure 2C. Two successive well-defined, reversible oxidation–reduction waves are observed, with formal potential values of $E^\circ_1 = 0.40$ and $E^\circ_2 = 0.55$ V vs SCE. A linear relationship of peak current with potential sweep rate v was observed, and the potential difference between the cathodic and anodic peak is smaller than 10 mV at scan rates of 0.1 V s^{-1} or less. These voltammetric features unequivocally indicate the surface-confined nature of the electroactive dendrimer film. To our knowledge, this is the first example of electrode surfaces modified with films of redox-active dendrimers possessing a controlled number of interacting metal centers.

In conclusion, we have shown that dendritic structures possessing organometallic units which are electronically communicated can be constructed in a simple convergent approach. This synthetic strategy provides also a versatile and promising access to heterometallic dendrimers, whose construction is in progress.

Acknowledgment. We thank the Dirección General de Investigación Científica y Técnica (Project No. PB-93-0287) for financial support of this research. We are grateful to Dr. David Tudela (Universidad Autónoma de Madrid) for helpful discussions.

Supporting Information Available: Detailed synthetic and electrochemical procedures, complete spectroscopic data for **1**–**6**, and further details of the crystal structure of **1** (21 pages). See any current masthead page for ordering and Internet access instructions.

JA971496W

(8) Richardson, D. E.; Taube, H. *Inorg. Chem.* **1981**, *20*, 1278.

(9) (a) Robin, M. B.; Day, P. *Adv. Inorg. Chem. Radiochem.* **1967**, *10*, 247. (b) Creutz, C. *Progr. Inorg. Chem.* **1983**, *30*, 1.